Int. J. Electrochem. Sci., 10 **(2015)** 1574 - 1581

International Journal of
ELECTROCHEMICAL
SCIENCE
www.electrochemsci.org

Short Communication

Electrodeposited Nickel Hydroxide on the Reduced Graphene Oxide with High Capacitance

Zixiang Yang[1,2], *Chunhui Fang*[2,*], *Yan Fang*[2,*], *Yongquan Zhou*[1], *Fayan Zhu*[1]

[1]Key laboratory of Salt Lake Resources and Chemistry, Institute of Salt Lakes, Chinese Academy of Sciences, Xining, Qinghai 810008, China
[2]University of the Chinese Academy of Sciences, Beijing, 100049
[*]E-mail: fangch@isl.ac.cn

Received: 4 November 2014 / *Accepted:* 18 December 2014 / *Published:* 30 December 2014

Electrochemical catalytic oxidation, a simple, green, novel and cost-effective approach to obtain graphene oxide, is introduced for the preparation of graphene oxide nanosheet-modified electrode. After reduced by the electrochemistry method, we can clearly see the graphene structure according to the FE-SEM. Nickel hydroxide, a low cost, high theoretical capacitance, ready availability and green supercapacitive material, is deposited into the reduced graphene oxide nanosheets without adding any other binder or metallic current collector. The composite materials exhibit a specific capacitance of 1700 F/g at a charge and discharge current density of 5 A/g and 967 F/g at 20 A/g with excellent cycling ability. Meanwhile, the electrode exhibits an excellent specific capacitance of 950 F/g at a charge and discharge current density of 5 A/g after 500 cycle tests. These results suggest a novel pathway to synthesize the graphene oxide for high-performance energy applications after being reduced.

Keywords: graphene; nickel hydroxide; electrocatalytic oxidation; supercapacitor; electrodeposition

1. INTRODUCTION

Over the past a few years, supercapacitors, which store energy by forming a double layer of electrolyte ions and are not limited by the electrochemical charge transfer kinetics just as batteries [1], have raised considerable attention as one of the most important types for next–generation energy storage devices due to its high power performance, short charging discharging time, excellent cycling stability, and low maintenance cost. There are two types of supercapacitors, electrical double-layer capacitors and pseudo capacitors originated from quick Faradaic charge transfer reactions, which are divided based primarily on their charge-storage mechanism [2,5]. Generally, electrical double-layer

capacitors mainly depending on the carbon materials achieve relatively low specific capacitance [6]. In this case, the specific capacitance or energy density of supercapacitor is too low to meet the ever-growing need and to achieve their use of full-scale range [7]. Pseudo capacitors based on conducting polymers and metal oxides can offer much higher specific capacitance than that of the electrical double-layer capacitors. The emergence of the asymmetric supercapacitor, where fast and reversible faradic processes occurs due to electro-active species [8], establishes on the concept between the battery and capacitor which can promote the energy density to a higher level and also keep the adventages such as the cycle life and power density of the supercapacitor well [9]. So Metal oxides, polymers, and hydroxides as the active materials of typical pseudocapacitive have always been studied [10-14].

Among various 'pseudoactive' materials, $Ni(OH)_2$ is an promising candidate for high performance supercapacitors because of its high specific capacitance and well-defined redox transitions [15]. However, the poor conductivity of $Ni(OH)_2$ limits the fast electron transfer contributed to a high power density [16]. Fortunately, graphene, one emerging and extraordinary carbon nanostructure, is a wonder material which brings new perspectives and prospects in many fields with many superlatives such as high surface area and electrical conductivity [17,18]. And with these properties the graphene can improve the fast electron transfer to a great extent especially as a conductive additive into the $Ni(OH)_2$ electrode [19]. In 2010, Dai et al. produced a highly conducting graphene sheets oxidized lightly.

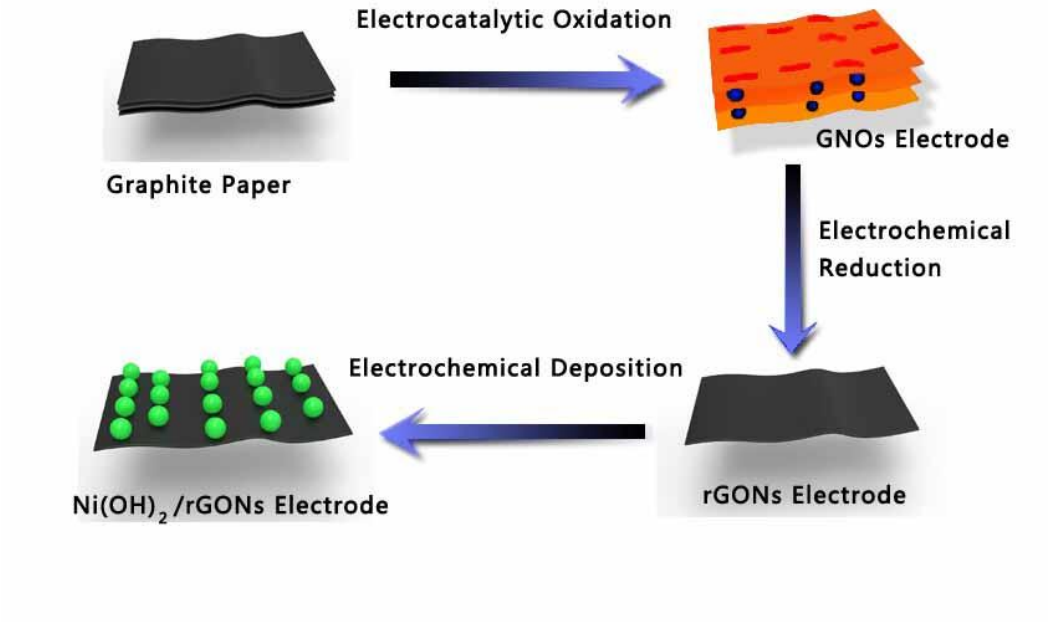

Scheme 1. Process of the Preparation of the $Ni(OH)_2$ /rGONs Electrode

And they were successful to grow $Ni(OH)_2$ on graphene by a two-step method, which exhibited a high specific capacitance of ~1335 F/g at a charge and discharge current density of 2.8 A/g [20]. They also pointed out that the degree of the oxidation of the graphene could play an important role in

the pesudocapacitance and rate capability of the composite materials. Suitable oxygen-containing functional groups on graphene sheet might be attributed to the pseudo capacitance of many metal materials [21]. But higher oxygen content leads to the reduction of the conductivity of the electrode material [22].

Graphite paper is a promising material for the application as the electrode with a sheet thickness of 0.05 mm. As is mentioned in the above scheme, we present a novel method for the preparation of graphene oxide nanosheet-modified electrode from the treatment of the graphite paper by electrochemical catalytic oxidation.

2. EXPERIMENTAL SECTION

2.1. Preparation of graphene oxide nanosheets and reduced graphene oxide nanosheets

The graphite paper was bought from Beijing graphite factory. A potential of 10 V was applied between the graphite paper (about 1*1 cm) for positive electrode and graphite electrode as cathode by constant potential electrolysis in an aqueous Na_2SO_4 (about 0.493 mol/L) solution. NaCl as the catalyst was also added into the solution with the concentration 0.862 mol/L. The whole electrolytic process lasted about 1 hour and we can get the modified GONs electrode. The GONs was reduced by cyclic voltammetry (-1.5~0.5, 10 mV/s) in 0.2 mol/L phosphate buffered solution (pH=6.8) in a three-electrode cell with the graphite and the calomel electrode (1 mol /L) as the counter and reference electrode.

2.2. Preparation of the graphite/$Ni(OH)_2$ and rGONs/$Ni(OH)_2$ electrode

With the rGONs-modified electrode as working electrode, graphite as counter electrode, and an 1 mol /L calomel electrode as reference electrode, $Ni(OH)_2$ nanoflakes were electrodeposited lasted about 1000 s on the graphite paper and rGONs-modified electrode in $Ni(NO_3)_2$ solution in the potential of -0.7 V.

2.3. Structure characterization and electrochemical measurements

The morphologies of rGONs and rGONs/$Ni(OH)_2$ nanoplates were characterized by FE-SEM (SU8010，Hitachi Limited in Japan). And the C/O atomic ratio of GONs is obtained by EDS. For electrochemical measurements, CV and galvanostatic charge and discharge were carried out on an Autolab electrochemistry workstation (AUT85048).

3. RESULTS AND DISCUSSION

By using constant potential electrolysis at anodic potentials (10 V in a aqueous solution containing Na_2SO_4 and NaCl as the catalyst) [23], The catalyst anion Cl^- is getting close to the anode

under a strong electric field with the strong anion oxidant such as ClO^- generated, and in this process the strong anion oxidant reacts with graphite to produce graphite oxide nanosheets(GONs). We are successful to obtain the GONs-modified electrode easily which avoids the trouble of the preparation of electrode and enlarges the activated surface area of GONs-modified electrode as much as possible [24]. The *van der Waals* force between graphitic sheets is weakened by the electrochemical catalytic oxidation and GONs are thus formed. An electrochemical method was carried out to reduce the GONs. The electrochemical reduced GONs, referred to as rGONs herein, was applied with cyclic voltammetry in 0.2 M phosphate buffered solution [25]. To prepare $Ni(OH)_2$ nanoflakes on graphite paper and rGONs-modified electrode, a potential of -0.7 V was applied in $Ni(NO_3)_2$ solution [26].

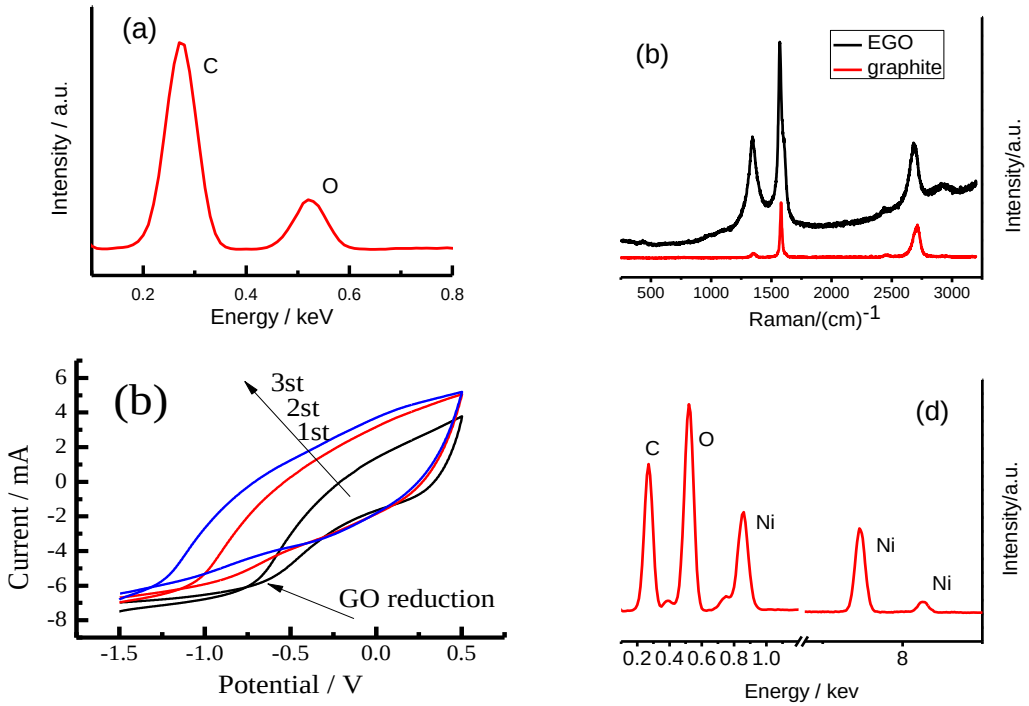

Figure 1. EDS characterization (a), Raman (b) and CV (c, three cycles) of GONs, and EDS characterization (d) of rGONs/$Ni(OH)_2$

As is shown in Figure 1(a), the GONs are investigated by EDS, which reveals that the nanocomposite is mainly composed of C and O. And according to the EDS, the C/O atomic ratio of the GONs is 3.8, which is higher than the graphene oxide produced by chemical method but it is dramatically decreased compared to graphite. It reveals that the GONs have experienced a certain degree of oxidation. Figure 1（b） records the Raman spectral of the EGO and graphite. We can clearly observe that the intensity ratio I_D / I_G of 0.55 was significantly lower than that of GO, which means the EGO has low defect content. The CVs in Figure 1(c) reveal the reduction process of the GONs. In the first cycle, there is a mild reduction peak around -0.75 V attributed to electrochemical reduction of GONs. As the potential cycling goes, the reduction peak disappears completely in the next two cycles indicating the process is not reversible. Besides, the area of the CV curves increases with

the reduction cycles under the same condition, which shows the rGONs has a better capacitance after being reduced. EDS characterization of rGONs/$Ni(OH)_2$ revealed in Figure 1(d) confirm that $Ni(OH)_2$ has been electrodeposited successfully. It also means the capacitance of the GONs turns bigger, which shows the rGONs has a better capacitance after being reduced. The specific capacitance C from the CV can be calculated based on the following equation:

$$C = \frac{S}{2mkV} \qquad (1)$$

Where C is the specific capacitance (F/g), S is the area of the CV curves, m is the mass of active material, k is the scan rates of the CV, and V is the potential window.

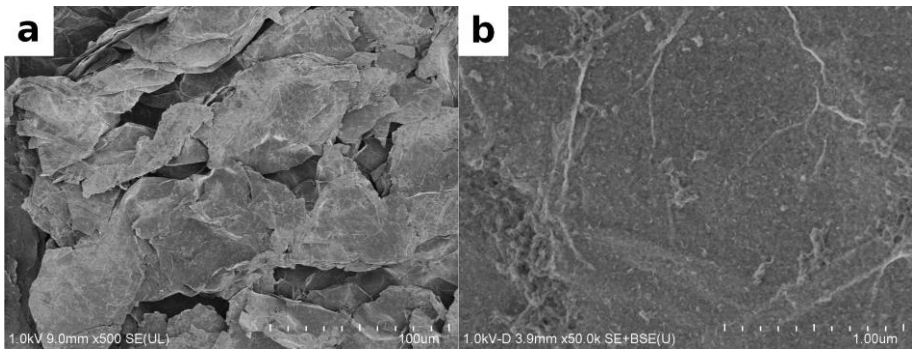

Figure 2. SEM images of rGONs (a) and rGONs/$Ni(OH)_2$ (b)

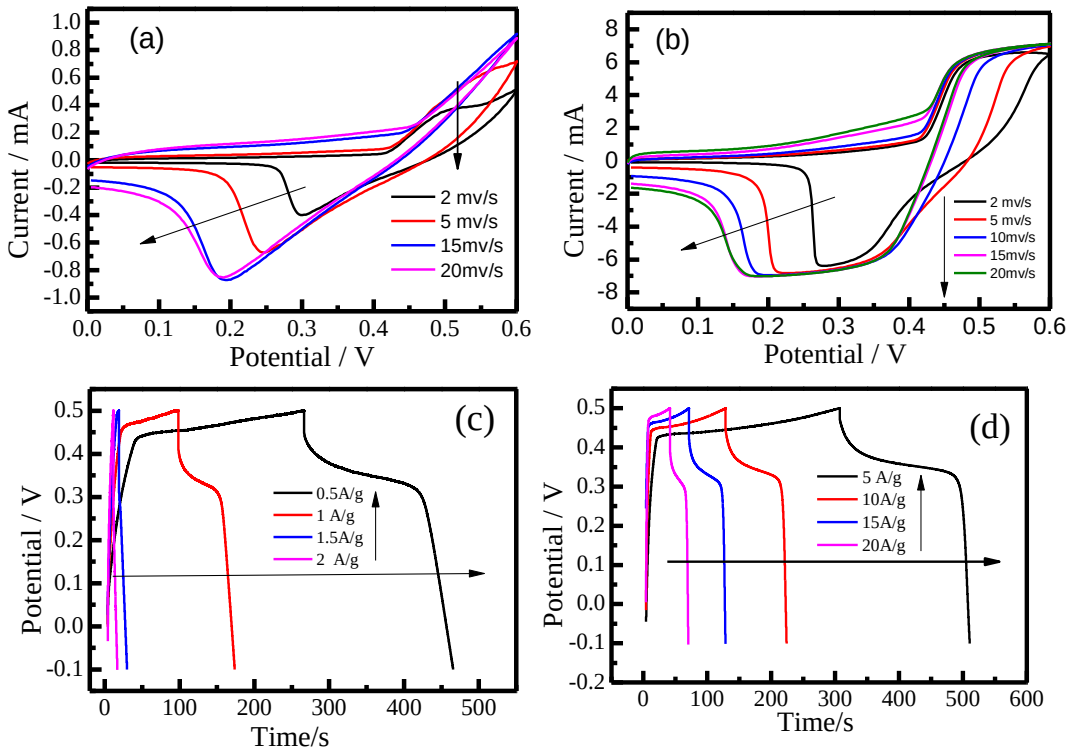

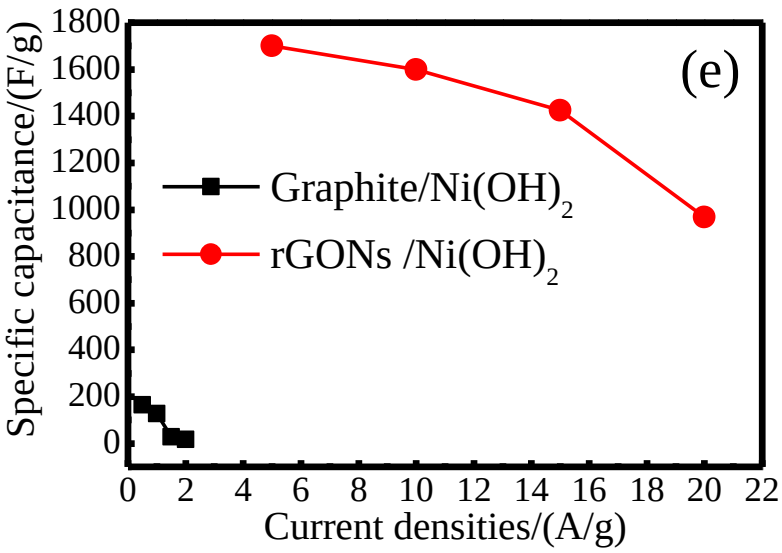

Figure 3. CV curves of $Ni(OH)_2$/graphite composite(a) and $Ni(OH)_2$/rGONs composite(b) at various scan rates in 1M KOH; Galvanostatic charge and discharge curves of $Ni(OH)_2$/graphite (c)and $Ni(OH)_2$/rGONs composite (d); Average specific capacitance of $Ni(OH)_2$/graphite and $Ni(OH)_2$/rGONs composite (e) at various discharge current densities.

The morphology of the rGONs and rGONs/$Ni(OH)_2$ electrode is characterized by using SEM. After the treatment of the electrochemical oxidation, there are clearly thin and large-sized graphitic sheets generated on the electrode surface intrinsic to the graphene in Figure 2(a). Also in the Figure 2 (b) the image further illustrates the uniform growth of $Ni(OH)_2$ on graphene sheets.

Figure 3 (a) and (b) show the CV curves of the graphite paper/$Ni(OH)_2$ and rGONs/$Ni(OH)_2$ electrode at different scan rates. All the curves have a pair of redox peaks which suggest that the specific capacitance of these composite is mainly contributed by pseudo capacitive capacitance [29]. On the other hand, these curves also show a well combination of both pseudocapacitive and double electrode layer types of capacitance. The anodic peak observed around 0.45 V is attributed to the oxidation process of $Ni(OH)_2$ to NiOOH, whereas the cathodic peak around 0.2 V is related to the reverse reduction process [30]. At the same time, the shapes of these CV curves have almost no significant change meaning excellent electron conduction and small equivalent series resistance with the increasing of the scan rates.

Figure 3 (c) and (d) show the constant current charge-discharge behavior of the electrodeposited Ni(OH)2 on the graphite and rGONs. The specific capacitance of the graphite/Ni(OH)2 and rGNOs/Ni(OH)2 can be calculated by the following equation:

$$C = \frac{I\Delta t}{m\Delta V} \quad (2)$$

Here, I is the applied current density, Δt is the discharging time, m is the mass of Ni(OH)2 electrodeposited in the electrode, and ΔV represents the discharge voltage range.

According to Equation (2), the specific capacitance values of the rGNOs/$Ni(OH)_2$ electrode calculated from the galvanostatic charge and discharge curves were 1700, 1600, 1425 and 967 F/g at the current densities of 5, 10, 15 and 20 A/g at a potential range of -0.1~0.5, respectively. The charge-

discharge measurements with large current densities mean more precisely the performance of the supercapacitor for an instant supply of power. And through the comparison of the specific capacitance, we can see that the specific capacitance has greatly improved after the electrochemical treatment of the graphite.

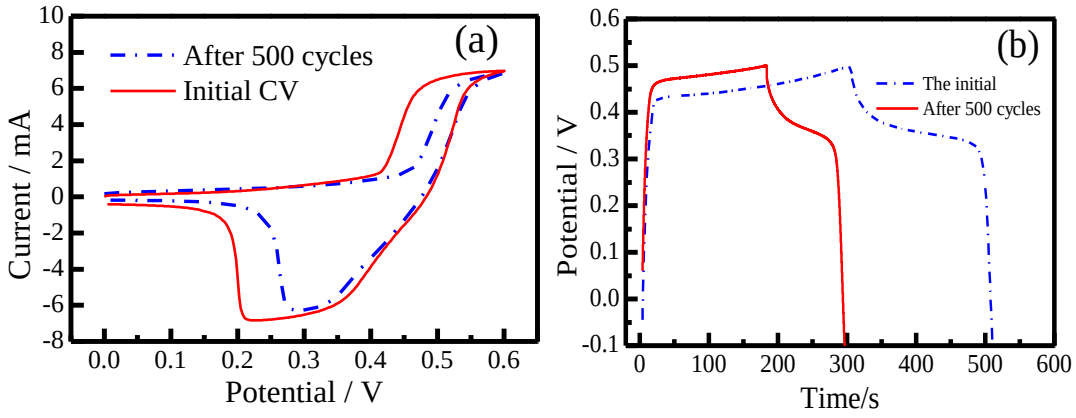

Figure 4. The CV curves of the the rGNOs/Ni(OH)$_2$ before and after 500 cycles at 5 mV/s (a). The galvanostatic charge-discharge curves of the rGNOs/Ni(OH)$_2$ before and after 500 cycles at 10 A/g(b).

As shown in figure 4, the CV and constant current charge-discharge cycling tests were used to measure the difference of the rGNOs/Ni(OH)$_2$ before and after 500 cycles. The repetitive charge/discharge of 500 cycles is applied at a current density of 20 A/g, which induces degradation of the electrode and results in some discharge specific capacitance loss due to the active materials falling off. Figure 4(a) shows there is an obvious potential difference [31], which can be used as a measure of the reversibility of the redox reaction and the relatively small value means better reversibility [32]. At the same time, Figure 4(b) shows the galvanostatic charge-discharge curves of the rGONs/Ni(OH)$_2$ electrode before and after 500 cycles. We can clearly observe that the charge-discharge time is shorter after 500 cycles, which means that the specific capacitance turns smaller.

4. CONCLUSIONS

In summary, graphene oxide nanosheets are successfully synthesized by the electrocatalytic oxidation and can be reduced in situ by the electrochemical method in the present paper. The reduced graphene nanosheets modified electrode after being anchored by Ni(OH)$_2$ exhibits a high specific capacitance of 1700 F/g at a charge and discharge current density of 5 A/g and 967 F/g at 20 A/g. At the same time, we avoid the process of the electrode preparation without the addition of binder. The structure is used as the current collector to greatly improve the electric conductivity compared with the ordinary current collector. This study opens up a new pathway to achieve the promising energy and power densities as electrode material of supercapacitors.

ACKNOWLEDGEMENTS
This research was supported by the National Science Foundation (Grant Number: 21373251) and the Main Direction Program of Knowledge Innovation of Chinese Academy of Sciences (Grant Number: KZCX2-EW-307).

References

1. Y. Zhu, S. Murali, M. D. Stoller, K. J. Ganesh, W. Cai, P. J. Ferreira, A. Pirkle, R. M. Wallace, K. A. Cychosz, M. Thommes, D. Su, E. A. Stach and R. S. Ruoff, *Science*, 332 (2011) 1537.
2. H. B. Li, M. H. Yu, F. X. Wang, P. Liu, Y. Liang, J. Xiao, C. X. Wang, Y. X. Tong and G. W. Yang, *Nat. Commun*., 4 (2013) 1894.
3. M. Winter and R. J. Brodd, *Chem. Rev*., 105 (2005) 1021.
4. D. A. Corrigan and R. M. Bendert, *J. Electrochem. S*., 136(1989) 723.
5. H. Zhang, X. Zhang, D. Zhang, X. Sun, H. Lin, C. Wang and Y. Ma, *J. Phys. Chem*. B , 117 (2012) 1616.
6. Z. Sun and X. Lu, *Ind. Eng. Chem. Res*., 51 (2012) 9973.
7. H. Chen, L. Hu, M. Chen, Y. Yan and L. Wu, *Adv. Funct. Mater*., 24 (2014) 934.
8. L. L. Zhang and X. S. Zhao, *Chem. Soc. Rev*., 38 (2009) 2520.
9. R. F. Service, *Science*, 313 (2006) 902.
10. G. Zhou, D.-W. Wang, L.-C. Yin, N. Li, F. Li and H.-M. Cheng, *ACS Nano*, 6 (2012) 3214.
11. Y. Liang, H. Wang, H. Sanchez Casalongue, Z. Chen and H. Dai, *Nano. Res*. 3 (2010) 701.
12. R. Liu and S. B. Lee, *JACS*, 130 (2008) 2942.
13. H. Wang, H. S. Casalongue, Y. Liang and H. Dai, *JACS*, 132 (2010) 7472.
14. Z. Wu, X.-L. Huang, Z.-L. Wang, J.-J. Xu, H.-G. Wang and X.-B. Zhang, *Sci. Rep*. 4 (2014) 3669.
15. J. Ji, L. L. Zhang, H. Ji, Y. Li, X. Zhao, X. Bai, X. Fan, F. Zhang and R. S. Ruoff, *ACS Nano*, 7 (2013) 6237.
16. X. Wang, Y. Wang, C. Zhao, Y. Zhao, B. Yan and W. Zheng, *New J. Chem*., 36 (2012) 1902.
17. A. Ambrosi, C. K. Chua, A. Bonanni and M. Pumera, *Chem. Rev*. ,(2014).
18. A. K. Geim, Science, 324(2009) 1530.
19. S. Min, C. Zhao, G. Chen and X. Qian, *Electrochim. Acta*., 115 (2014) 155.
20. H. Wang, J. T. Robinson, G. Diankov and H. Dai, *JACS*, 132 (2010) 3270.
21. Y.-Y. He, J.-J. Zhang and J.-W. Zhao, *Acta. Phys. Chim. Sin*., 2 (2014) 297.
22. F. Zeng , Z. Sun, X. Sang, D. Diamond, K. T. Lau, X. Liu and D. S. Su, *ChemSusChem*, 4 (2011) 1587.
23. L.-X. Zhu, Y.-Z. Li, X, Zhao and Q.-H Zhang, *Chem. J. Chinese* U., 33 (2012) 1804.
24. Z. Wang, X. Zhou, J. Zhang, F. Boey and H. Zhang, *J. Phys. Chem.* C, 113(2009) 14071.
25. Z.-Z. Zhao, W.-B. Ni, N.-Y. Gao, H.-B. Wang and J.-W. Zhao, *Electrochemistry*, 17(2011) 292.
26. H.-C. Chien, W.-Y. Cheng, Y.-H. Wang and S.-Y. Lu, *Adv. Funct. Mat*., 22(2012) 5038.
27. D. R. Dreyer, S. Park, C. W. Bielawski and R. S. Ruoff, *Chem. Soc. Rev*., 39 (2010) 228.
28. Y. Shao, J. Wang, M. Engelhard, C. Wang and Y. Lin, *J. Mater. Chem*., 20 (2010) 743.
29. J. Yan, Z. Fan, W. Sun, G. Ning, T. Wei, Q. Zhang, R. Zhang, L. Zhi and F. Wei, *Adv. Funct. Mat.*, 22 (2012) 2632.
30. Y. Zhang, F. Xu, Y. Sun, Y. Shi, Z. Wen and Z. Li, *J. Mater. Chem*., 21(2011) 16949.
31. G.-W. Yang, C.-L. Xu and H.-L. Li, *Chem. Comm*. ,48 (2008) 6537.
32. F.-S. Cai, G.-Y. Zhang, J. Chen, X.-L. Gou, H.-K. Liu and S.-X. Dou, *Angew. Chem. Int. Edit*., 43(2004) 4212.